Results in Engineering 21 (2024) 101797

Contents lists available at ScienceDirect

Results in Engineering

journal homepage: www.sciencedirect.com/journal/results-in-engineering

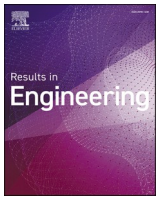

The impact of waste brick and geo-cement aggregates as sand replacement on the mechanical and durability properties of alkali–activated mortar composites

Eslam El-Seidy [a], Mehdi Chougan [a], Yazeed A. Al-Noaimat [a], Mazen J. Al-Kheetan [b], Seyed Hamidreza Ghaffar [a,c,d,*]

[a] Department of Civil and Environmental Engineering, Brunel University, London, Uxbridge, Middlesex, UB8 3PH, United Kingdom
[b] Department of Civil and Environmental Engineering, College of Engineering, Mutah University Mutah, Karak, 61710, P.O. BOX 7, Jordan
[c] Applied Science Research Center, Applied Science Private University, Jordan
[d] Department of Civil Engineering, University of Birmingham, Dubai International Academic City, Dubai, P.O. Box 341799, United Arab Emirates

ARTICLE INFO

Keywords:
Alkali-activated materials
Waste brick
Waste geo-cement
Aggregates
Durability

ABSTRACT

This study explores the potential of waste brick and geo-cement aggregates as substitutes for natural sand in alkali-activated materials (AAMs) for mortar production. With a focus on achieving net-zero construction and mitigating environmental impact, the study replaces Portland Cement (OPC) and virgin aggregates with waste materials and by-products. The investigation evaluates the substitution of sand (up to 100 % by weight) in AAMs with waste brick aggregates (WBA) and waste geo-cement aggregates (WGA) obtained from demolished construction and research lab waste, respectively. The research methodology involves assessing mechanical, durability, and microstructure properties to assess the performance of the developed AAMs with waste aggregates. Notably, AAM composites containing waste brick and geo-cement aggregates surpass natural aggregate composites in terms of mechanical strength, water absorption, freeze-thaw resistance, acid ingress, and chloride attack. The 7-day 50 % waste brick mixture achieved a maximum compressive strength of 61 MPa, while a 70 % waste geo-cement mortar mixture attained a maximum flexural strength of 12 MPa. Combinations, whether comprising waste brick or geo-cement mortar aggregates, demonstrate compressive strengths well over 40 MPa, rendering them suitable for heavy load-bearing structures. The 50 % waste geo-cement mortar mixture stands out with the lowest water absorption rate of 6 % and the least compressive strength loss of 13 % after the freeze-thaw test, with reductions of 6 % and 18 %, respectively, compared to the control. Additionally, 100 % waste brick AAMs exhibit the lowest compressive strength loss after chloride and acid attack tests, with reductions of 13 % and 2.5 %, respectively. When compared to all other mixtures, the 50 % waste brick aggregates mortar mixture obtained the best overall performance. The composites developed in this study affirm their suitability for use in heavy-load structural components, showcasing favourable mechanical and durable properties. These findings underscore the need for additional exploration in this direction to advance sustainable construction practices.

1. Introduction

Circular economy (CE) is an economic system that involves reducing, reusing, recycling, and recovering materials throughout the production, distribution, and consumption of "end-of-life" products [1]. Implementing CE strategies can help mitigate global warming and environmental impacts caused by the construction industry, which is responsible for approximately 36 % of global carbon emissions, rising to 40–50 % in industrialised countries [2]. Cement manufacturing, which is responsible for 8 % of worldwide CO_2 emissions, significantly contributes to the construction industry's environmental impact, producing approximately 2.083 billion tonnes of CO_2 annually. If the current rate of emissions is maintained, emissions from the cement sector are expected to reach 2.34 billion tonnes annually in 2050 [3,4]. The predicted CO_2 reductions in relation to AAMs and Portland cement ranged from 9 % to 97 %. The exact alkali-activated binder mix design, the curing conditions used, the properties of the reference Portland cement system, and geographical concerns connected to material availability and

* Corresponding author. Department of Civil and Environmental Engineering, Brunel University, London, Uxbridge, Middlesex, UB8 3PH, United Kingdom.
E-mail address: seyed.ghaffar@brunel.ac.uk (S.H. Ghaffar).

https://doi.org/10.1016/j.rineng.2024.101797
Received 2 October 2023; Received in revised form 11 January 2024; Accepted 12 January 2024
Available online 14 January 2024

transportation all affected these variances [5]. One of the perplexing issues within the researchers studying alkali-activated binders revolves around the extensive spread of various terms denoting essentially the same material. This nomenclature encompasses a wide range of designations, including "alkali-bonded ceramic," "alkali ash material", "geo--cement", "geopolymer", "hydro-ceramic", "inorganic polymer", "mineral polymer", "soil cement", "soil silicate", among others [6]. The construction industry also consumes a large percentage of natural resources, for instance, it consumes about 49 % of raw stone, gravel, and sand, 25 % of virgin wood, and 16 % of water [7]. As the demand for river sand in the construction industry continues to grow, natural resources are being depleted and the environment is being negatively affected, e.g. the decrease in the water table of rivers and erosion of riverbanks [8]. Therefore, employing alternatives to cement and natural aggregates, such as alkali-activated binders and construction and demolition waste (CDW), in the concrete manufacturing sector is imperative, as they can significantly reduce CO_2 emissions while also improving mechanical and durability properties [9]. CDW is composed of bulky and heavy materials such as concrete, wood, asphalt, gypsum, metals, bricks, glass, plastics, soil, and rocks. Approximately 35 % of the world's CDW is landfilled or illegally disposed of, which poses significant environmental concerns and increases waste disposal costs [10,11]. According to the US Environmental Protection Agency's advanced sustainable materials management reports, 600 million tonnes of CDWs were created in the United States in 2018. In 2016, the European Union (EU-28) generated 374 million tonnes of CDWs (excluding excavated soil), the biggest waste stream (by mass) [12]. Moreover, bricks are the second most frequently used building material after concrete, forming a significant portion of the world's CDW. They are classified as Construction and Demolition (C&D) debris as they sustain damage during the production, construction, or demolition processes [13]. Ground clay brick is widely regarded as a pozzolanic material, where SiO_2, Al_2O_3, and Fe_2O_3 form over 70 % of its constituents, satisfying the ASTM C618 criterion [13]. Brick masonry is used to construct nearly all residential structures in the subtropical region, and 1391 billion bricks are produced globally every year [14]. Moreover, each year, the European Union and the United States produce roughly 800 and 700 million metric tonnes of CDW, respectively. China, the world's largest developing nation, generates approximately 1.8 billion metric tonnes of construction and demolition waste annually. Approximately 80 % of the total CDW is comprised of brick and concrete waste [15]. Additionally, M. Ngoc-Tra Lam et el. (2023) [16] reported that about 54 % of the CDW is composed of clay bricks and ceramic materials.

While the construction industry is still in the early stages of assessing the viability of geopolymers, understanding the prospective challenges in dealing with geopolymers' waste at the end-of-life of geopolymers concrete requires special attention [17]. Mesgari et al. [17] assessed the use of geopolymer waste aggregates in geopolymer and OPC- based mixtures as coarse aggregates with a size of 12 mm, where four replacement ratios were considered; 0, 20, 50, and 100 % of the weight of natural coarse aggregates. They found that waste geopolymer aggregates gave better results, at all replacement ratios, when incorporated in the geopolymer concrete compared to OPC concrete in terms of mechanical properties. In another study by Tavakoli et al. [18], natural sand in OPC-based concrete was replaced by waste clay brick aggregates at five replacement ratios: 0, 25, 50, 75, and 100 %. They indicated that concrete with 25 % waste clay brick aggregates obtained the highest compressive strength of 43 MPa at 28 days, attributed to the waste clay brick aggregates' pozzolanic activity, which enhances the bonding between aggregates and the paste. However, incorporating waste clay brick aggregates in higher ratios than 25 % was found to negatively affect the strength of concrete due to the porous structure of waste clay brick aggregates and the development of cracks. Atyia et al. [19] reached a similar conclusion that the inclusion of high ratios of clay waste brick as fine or coarse aggregates in OPC-based composites weakened their mechanical properties. This was attributed to the weaker nature of waste clay aggregates and higher water absorption compared to natural aggregates. In a study carried out by C. Wang et al. [20] to introduces fibre-reinforced recycled aggregate concrete (FRAC) to address issues like low toughness and cracking in recycled aggregate concrete. By incorporating steel fibre (SF) and polypropylene fibre (PPF) into the RAC matrix, the research provides experimental results on FRAC's behaviour under cyclic compression, focusing on damage growth and residual strain. The study proposes a constitutive model that accurately predicts FRAC's performance, considering fibre content. The findings offer valuable insights into enhancing the mechanical properties of recycled aggregate concrete, particularly in low cycle loading scenarios. Moreover, C. Wang et al. [21]conducted cyclic compressive tests on various fibre-reinforced recycled aggregate concrete (FRAC) formulations, exploring their hysteresis and damping properties. The study examined steel fibre (SF)-reinforced natural aggregate concrete (SF-R-NAC), SF-reinforced RAC (SF-R-RAC), and polypropylene fibre (PPF)-reinforced RAC (PPF-R-RAC) with different fibre contents. Key findings include the exploration of residual strain development, a proposed modified stress–strain constitutive model, and an analysis of FRAC's hysteretic characteristics, such as strain energy and viscous damping. The study introduced a novel viscous damping model, accounting for fibre content, and validated its effectiveness through predictions based on the modified constitutive model. C. Wang et al. [22] studied the use of a dynamic constitutive model for recycled aggregate concrete (RAC) to analyse the impact of strain rate and replacement ratio on structural restoring force behaviours, focusing on recycled coarse aggregate (RCA). It introduces a rate-dependent damage model for RAC frame structures and provides calculation models for characteristic parameters and strain rate influence factor models for various structural behaviours.

The principle of this research is to embrace circular economy strategies in cementitious composite production by exploring the potential of utilising waste brick and geo-cement as fine aggregates in alkali-activated formulations. Natural sand was replaced by waste materials in four replacement ratios of 0, 50, 70, and 100 %, and composites' mechanical, physical, microstructure, and durability properties were investigated to understand the behaviour of recycled aggregates and potential opportunity for reserving natural sand in cementitious composites. To the best of the authors' knowledge, this is the first research to incorporate waste brick and cement-free geo-cement mortar to completely replace natural sand aggregates in alkali-activated cementitious composites and to assess various durability tests. Despite the considerable number of studies conducted on the topic, there is a shortage of research specifically focused on geo-cement aggregates used in alkali-activated materials. Furthermore, there is a scarcity of studies that have fully (i.e., 100 %) replaced natural sand with waste brick and waste geo-cement aggregates in AAM systems. Our approach, which involves the development of low-carbon composites featuring zero cement and zero natural sand, while being suitable for a load-bearing structure and substantial durability, represents a groundbreaking step towards the implementation of a net-zero strategy.

2. Experimental framework

Fig. 1 explains the experimental methodology and characterisation procedures used in this study to explore the performance of low-carbon cementitious composites using waste aggregate replacements in detail.

2.1. Materials

The alkali-activated cementitious composites were prepared using (1) fly ash (FA) (Cemex, UK); (2) granulated blast furnace slag (GGBS) (Hanson Heidelberg Cement, UK) that abides with EN 15167-1; (3) micro-silica (MS) (J. Stoddard & Sons Ltd); (4) graded sand including two distinct sand sizes of 0–0.5 mm and 0.5–1.0 mm in accordance with BS EN 410–1:2000; (5) sodium silicate (Na_2SiO_3) solution with the SiO_2/

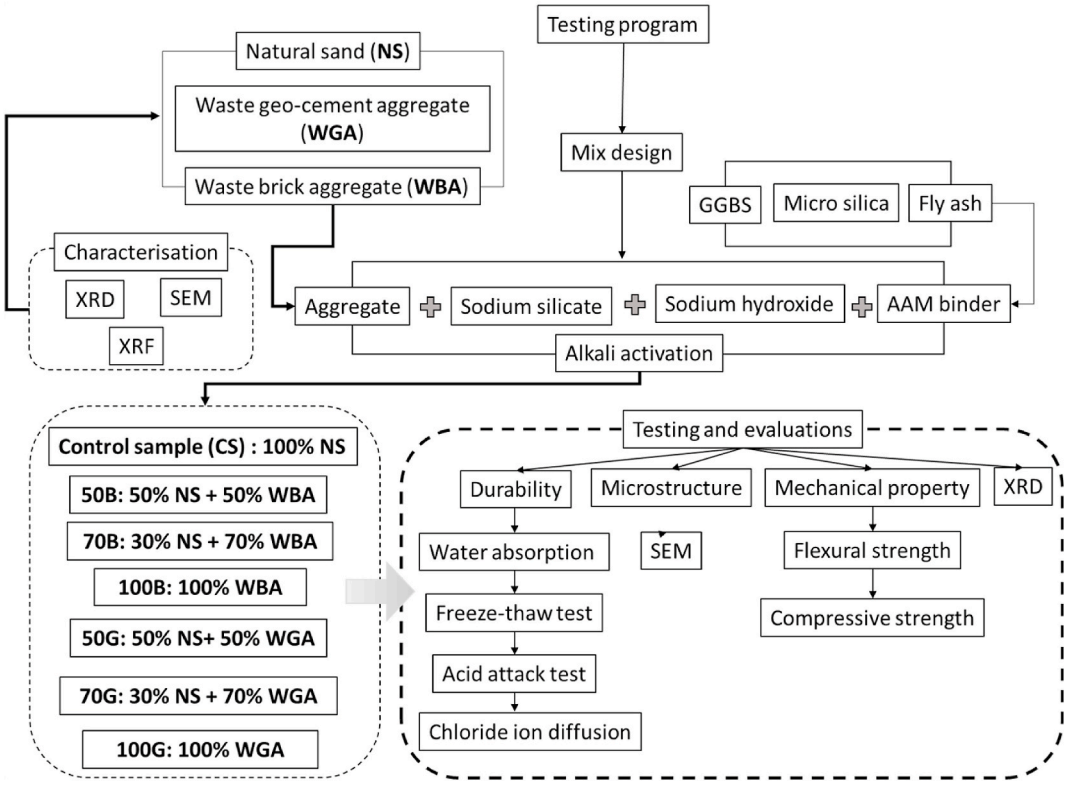

Fig. 1. The experimental design of the study.

Na_2O mass ratio of 3.0 (Solvay SA, Portugal); (6) 10 mol/l sodium hydroxide (NaOH) solution (Fisher Scientific, Germany); and (7) attapulgite nano clay additive with a fixed dose of 1 % by weight of binder (based on authors' prior research) [23]. The mix formulation has been developed by the authors from previous works based on several trials and errors [24,25]. Two type of waste aggregates were studied in this investigation, namely, waste brick aggregates (WBA) and waste geo-cement aggregates (WGA). Waste bricks were picked up from a demolished building on the Brunel University campus, cleaned and then manually broken into chunks and ground to a size of 1–2 mm using Retsch SM100 electric grinder. The waste geo-cement was collected from the cast specimens in the civil engineering laboratory at Brunel University, see Fig. 3. These geo-cements were cured at 60 °C for 24 h, left at room temperature for 6 days for testing in another research. The waste of these specimen was then manually broken down into smaller pieces, and then ground using the lab grinder to a size of 1–2 mm. The size of the aggregates was established by considering two factors: (1) the size of the local grinder's sieves and (2) minimizing energy consumption during the grinding process for finer aggregates. Fig. 2 illustrates the aggregates' microstructure and rough surface textures of (a) the waste brick aggregates consist of a combination of rounded and sharp-edged particles, while (b) the waste geo-cement aggregates exhibit angular edges with scattered notches on the surface. Table 1 illustrates the chemical composition of WBA and WGA. As shown in Fig. 4, several phases (i.e., Quartz (Q), Muscovite (MS), Carbon (C)) in both brick and geo-cement aggregates used in this study have been identified using XRD.

The high quantity of CaCO3 in WGA is due to the possibility of the

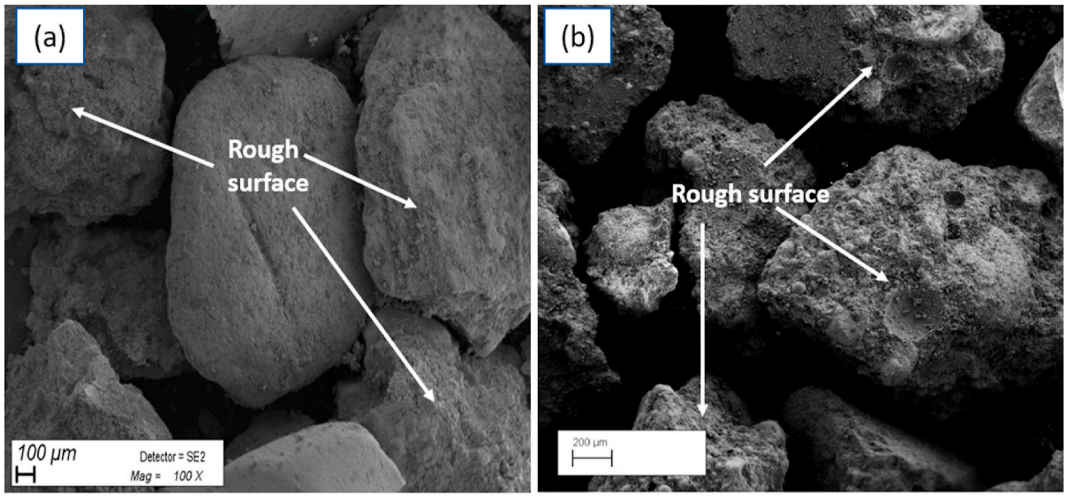

Fig. 2. Microstructure of (a) waste brick aggregates and (b) waste geo-cement aggregates.

Fig. 3. The process of obtaining WBA and WGA (a) chunks of bricks, (b) chunks of geo-cement, (c) The grinding machine, (d) grinding cylinder, (e) waste break aggregates, and (f) geo-cement aggregates.

Table 1
The chemical compositions of the WBA and WGA by X-ray fluorescence (XRF).

Material	SiO_2 (Wt. %)	$CaCO_3$ (Wt.%)	Al_2O_3 (Wt.%)	Fe_2O_3 (Wt.%)	P_2O_5 (Wt. %)	K_2O (Wt. %)
Waste brick aggregates (WBA)	74	0.761	12.7	6.56	2.69	1.79
Waste geo-cement aggregates (WGA)	52.6	15.4	9.65	4.91	2.86	1.2

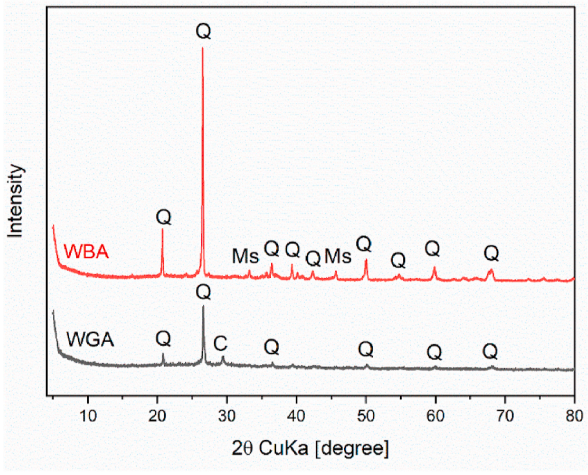

Fig. 4. XRD patterns of (a) waste brick aggregates and (b) waste geo-cement aggregates.

reaction of the CO_2 of the surrounding environment with the Cao of the GGBS [6].

2.2. Mix formulation and material preparations

A total of seven AAM mixes were prepared. The formulation of the control AAM mix (control sample - CS) detailed in Table 2, was chosen based on the authors' past research [23]. The chemical characterizations of the binders have been detailed in a prior publication by the authors [26]. At the outset, the precursor materials, which included FA, GGBS, SF, and aggregates (graded sand, WBA, and WGA), were dry mixed for 5 min at 250 rpm using a planetary mixer (Kenwood, Germany), maintaining a consistent binder-to-aggregates ratio of 0.8. In this study, 50 wt.-%, 70 wt.-%, and 100 wt.-% of natural sand aggregates was replaced with recycled aggregates (i.e., WBA and WGA). The establishment of replacement ratios is grounded in our prior research, wherein waste plastic aggregates (UPVC) were replaced up to 100 % [27]. Despite the inherent drawbacks associated with using plastic aggregate, we successfully attained commendable mechanical properties. Subsequently, this scientific groundwork provided the rationale to extend our investigation to mineral aggregates such as WGA (waste geo-cement aggregates) and WBA (waste brick aggregates) for complete substitution in lieu of sand. The alkali activator solutions (i.e., a mixture of 10 mol/l NaOH and Na_2SiO_3 with the SiO_2/Na_2O weight ratio of 3.23 and molar ratio of 3.3–3.5) with a mass ratio of 1:2 were mixed for 5 min using a magnetic stirrer, w/b ratio was 0.4 for all mixes. Finally, premixed alkali solutions were added gradually to the dry mixture, then mixed for 10 min at 450 revolutions per minute until homogenous AAM mixes with normal consistency and easy to spread and work with while maintaining proper cohesion, were obtained to produce mortar. AAM fresh mixes were cast using prismatic moulds with dimensions of 160 × 40 × 40 mm^3 for mechanical tests and metal cube moulds with dimensions of 50

Table 2
Mix formulation for AAM mixtures with waste brick aggregates (WBA) and waste geo-cement aggregates (WGA) at different replacement ratios.

Sample ID	Binder (wt.%)			Aggregate (wt.%)			
	FA	GGBS	Micro silica	Natural sand		Recycled aggregate	
				0–0.5 mm	0.5–1 mm	WBA	WGA
CS	60	25	15	60	40	0	0
50B	60	25	15	30	20	50	0
70B	60	25	15	18	12	70	0
100B	60	25	15	0	0	100	0
50G	60	25	15	30	20	0	50
70G	60	25	15	18	12	0	70
100G	60	25	15	0	0	0	100

× 50 × 50 mm^3 for durability tests (three samples for each mix) and put in an oven for 24 h at 60 °C (heat curing stage) followed by 6 days (air curing stage) at ambient temperature.

2.3. Experimental tests

2.3.1. Microstructure analysis

Microstructural analysis of alkali-activated materials (AAMs) was conducted utilising scanning electron microscopy (SEM) with a Supra 35VP instrument from Carl Zeiss, Germany. Each composition underwent analysis through at least ten samples, each measuring 8 mm^3 in size. Prior to SEM examination, all samples were subjected to gold coating using an Edwards S150B sputter coater to enhance electrical conductivity.

2.3.2. Mechanical properties

The mechanical performance of AAM samples (i.e., flexural, and compressive strengths) was assessed after 7 days of curing in accordance with BS EN 196–1:2016, using an Instron 5960 Series Universal Testing System. For each composite, three samples were tested for flexural strength and six samples for compressive strength. The loading rate was adjusted at 1 mm/min for both flexural and compressive tests in accordance with BS EN 196–1:2016.

2.3.3. Freeze-thaw test

Three cubes with the size of 50 × 50 × 50 mm^3 for each composite were frozen in cold air and thawed in water following the procedure of ASTM C666/C666 M. Freezing and thawing (F–T) temperatures were −20 °C and 20 ± 2 °C, respectively. Both the freezing and thawing timeframes were set to 12 h, indicating a single F–T cycle. In addition, the number of F–T cycles is 50. The degradation of the composites' mechanical characteristics due to F–T cycles was then examined in terms of mass loss and loss of compressive strength. Equations (1) and (2) were used to calculate the mass and the compressive loss.

2.3.4. Chloride attack test

This test was performed by immersing composites' samples in a saline solution, as per ASTM D114198. The samples with the dimensions of 50 × 50 × 50 mm^3 were immersed in tap water with 5 % sodium chloride for six weeks. Afterwards, all samples were dried, Subsequently, an analysis of the deterioration in the mechanical properties of the composite due to chloride penetration was conducted, focusing on the loss of compressive strength. the compressive strength loss was calculated followed the formula below:

$$Compressive\ strenght\ loss\ \% = \frac{\text{Initial compressive strength} - \text{Final comperssive strength}}{Initial\ compressive\ strength} \times 100 \quad (1)$$

Where, initial compressive strength is the compressive strength of a composites (MPa) after 7 days of curing, and the final compressive strength is the compressive strength of a composite (MPa) after conducted the Chloride test.

2.3.5. Acid attack test

The acid resistance of the cementitious samples with the dimensions of 50 × 50 × 50 mm^3 was assessed by exposing them to an acidic solution for 28 days. In line with ASTM C189820, the acidic solution was created by dissolving 5 % sulfuric acid in 40 L of tap water. After 28 days, the specimens were dried and weighed. The impact of acid attack on the mechanical properties of the composite was further examined, specifically in terms of weight loss and the reduction in compressive strength. the weight loss was calculated following the equation below:

$$Wieght\ loss\ \% = \frac{\text{Initial Weight} - \text{Final Weight}}{Initial\ Weight} \times 100 \quad (2)$$

Where, Initial weight is the composite's weight before the test (g), and final weight is the composite's weight after performing the acid attack test (g). To calculate the compressive strength loss, Equation (1) was applied.

2.3.6. Water absorption test for the composites

The conventional weight-measuring method following the ASTM C1585-13 procedure was used to assess the capillary water absorption of the composites. Each mixture was evaluated using a batch of three cubes, each measuring 50 × 50 × 50 mm^3. The specimens were placed in an oven at (60 ± 5 °C) until completely dry, after which the water absorption was measured at regular intervals over an eight-day period. Finally, the capillary water absorption rate of the composites was determined using the following formula:

$$Water\ absorption\ (\%) = \frac{M_t - M_0}{M_0} \times 100 \quad (3)$$

Where, M_0 (g) represents the oven-dried mass, and M_t (g) represents the saturated surface-dry mass.

2.3.7. Water absorption test for the aggregates

Water absorption (WA) is calculated as the ratio of the water needed to saturate a porous sample to its dry mass. The measurement involves drying the samples at a specified drying temperature (20 °C; 30 °C; 45 °C; 75 °C; 105 °C) to eliminate all water present in the pores (M_{dry}). Subsequently, the samples are immersed in water using a solid-to-liquid ratio of 100g to 1 L. The immersion is static, and the dissolution of the aggregates is considered slow, rendering leaching negligible [28]. After 24 h of water immersion, the samples are taken out of the water. Finally, the aggregate surface is meticulously dried with absorbent cloths until the water films on the aggregate surface vanish, achieving the "Saturated Surface Dry" (SSD) mass (M_{SSD}) in accordance with standard NF EN 1097-6 [29]. From these two measurements, the water absorption is calculated as:

$$\text{Water absorption}\ (\%) = \frac{M_{SSD} - M_{dry}}{M_{dry}} X\ 100 \quad (4)$$

3. Results and discussion

3.1. Mechanical characteristics

Fig. 5 displays the compressive and flexural strength results of AAM composites containing waste geo-cement and waste brick aggregates. It is evident that there are changes in the compressive and flexural strength of the specimen with recycled aggregates compared to the control sample. As shown in Fig. 5 a, the compressive strength values after incorporating WGA aggregates were reduced compared to the CS. The highest reduction of 23 % was obtained by the 70G sample. However, increasing the aggregate replacement percentages followed a reverse trend for flexural strength values. In a study conducted by Zhu et al. [30], the inclusion of more than 50 % recycled geopolymer aggregate in the metakaolin-based geopolymer system resulted in a noticeable

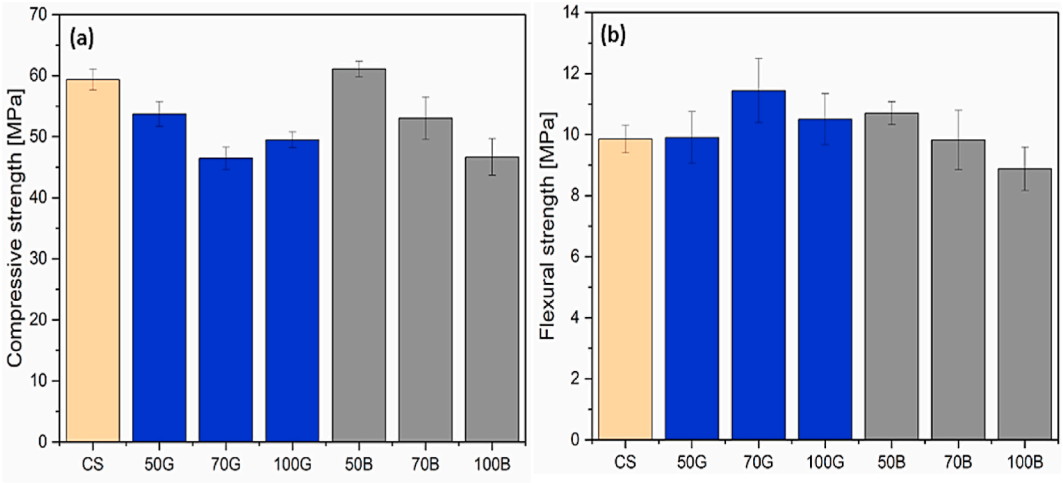

Fig. 5. (a) Compressive strength and (b) Flexural strength of the AAM composites with waste geo-cement (G) and waste brick (B) aggregates.

reduction in flexural and compressive strengths. Their results indicated that the reduction in compressive strength is associated with increased porosity of the composites, which is induced by the water absorption of the geopolymer aggregates, i.e., less available water in the system. However, the mechanical performance reduction rate is relatively milder than incorporating recycled mortar aggregates in a OPC-based cementitious system [30,31]. Compared to the value recorded for the control sample (i.e., 10 MPa), the flexural strength values first remained constant for 50G, then increased, and reached 12 MPa and 11 MPa for the 70G and 100G samples, respectively. The maximum flexural strength was about 12 MPa obtained for the 70G mixture, which was about 20 % higher than the CS. The modest increase in flexural strength in comparison to CS may be attributed to the bridging effect induced by WBA and WGA, thereby augmenting the flexural strength of the composites. This proposition finds support in a study conducted by G. Hauseien et al. [30], where ceramic waste powder from tiles (TCW) was integrated into alkali-activated composites utilising fly ash and ground granulated blast furnace slag (GGBS). The researchers noted that incorporating a substantial concentration of TCW led to minimal cracking, ascribed to the bridging effect of TCWs. This phenomenon heightened the capacity for energy absorption, mitigating the risk of sudden failure or collapse in the specimens. Another reason might be due to that WBA are driven from burnt clay bricks and then pulverized. The conventional brick kiln undergoes heating up to 1000–1500 °C, causing alumina, silica, and iron to transform into fused glass, serving as a binding agent for adhesion [32]. This stability leads to a stronger and more robust structure, providing the composites integrated with WBA with consistently superior mechanical behaviour compared to those with WGA. Conversely, WGA did not undergo exposure to such extreme temperatures, preventing the development of strong adherence in the WBA structure. As shown in Fig. 6, it is likely that the weaker structure of WGA experienced a somewhat inconsistent reaction during alkalisation, resulting in inconsistent mechanical behaviour.

The results indicated no obvious trend among composites containing WGA, on the other hand, composites containing WBA showed a declining of mechanical properties with the increasing of replacement ratios. For samples containing WBA, their compressive and flexural strengths slightly increased from 60 MPa to 10 MPa for CS and reached 61 MPa and 11 MPa for 50B. Subsequently, the compressive and flexural strengths gradually decreased to 52 MPa and 10 MPa for 70B and 45 MPa and 8 MPa for 100B, respectively.

The findings of this study align with the research conducted by Khattab et al. [33], which investigated the substitution of waste brick aggregates for natural aggregates in a Portland cement-based mortar. In both studies, a complete replacement of natural sand led to a decrease in compressive strength, amounting to a 22 % reduction. This decline was ascribed to the heightened porosity observed in the structure of the mortar. The compatibility between WBA and WGA aggregates and the binder was confirmed by examining the composites' microstructure (Fig. 7 (**a** and **b**) and (**c** and **d**)). Fig. 2 also verified the obtained results by revealing that both aggregates utilised in this investigation have comparable rough surface textures, which played a crucial role in

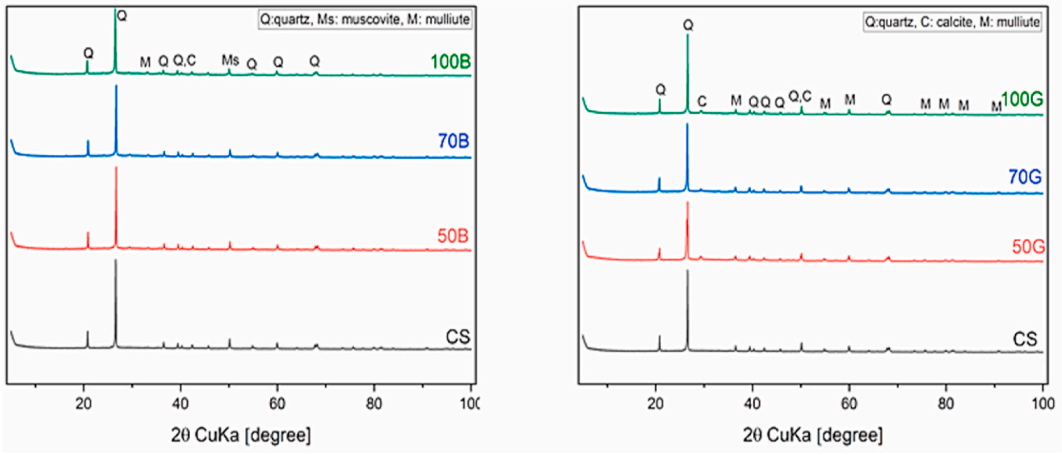

Fig. 6. XRD patterns of the AAM composites with (a) waste brick and (b) waste geo-cement aggregates.

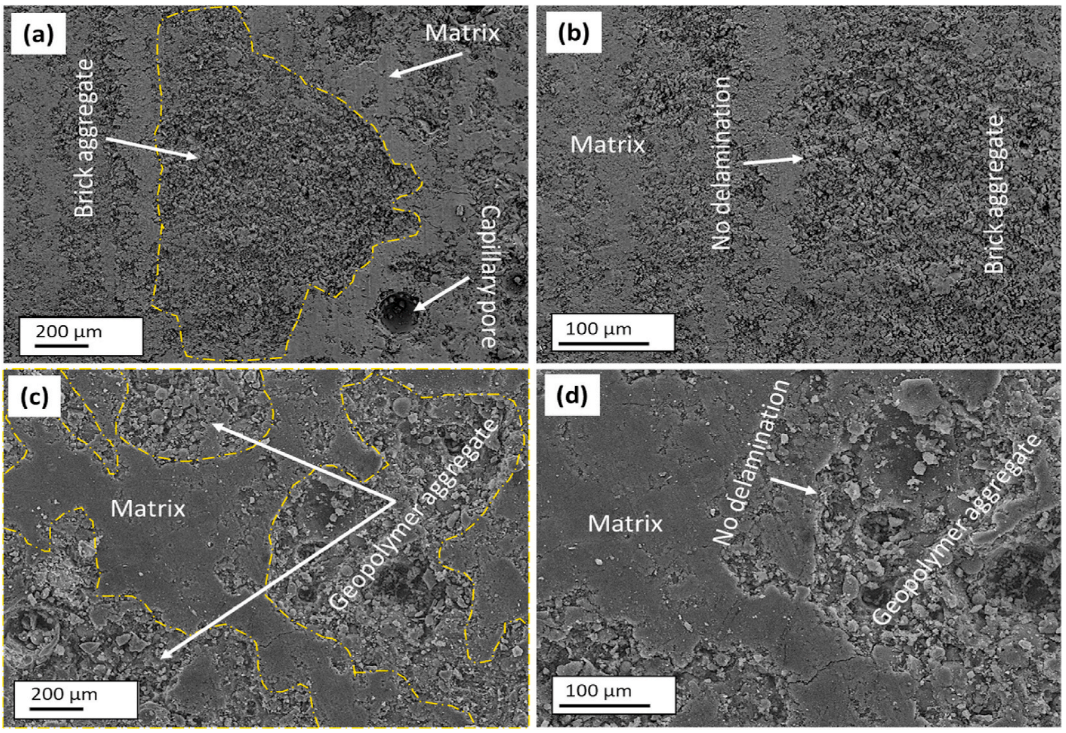

Fig. 7. Microstructure of (a) and (b) AAM composite with WBA, and (c) and (d) AAM composite with WGA.

aggregate and cement paste interlocking bonds. The rough surfaces and similar shapes of the waste aggregates to natural aggregate facilitated the bonding between waste aggregates and the mortar, leading to a cohesive composite with dense microstructure.

Regarding WBA, Olofinnade et al. [34] stated that based on the chemical composition of clay brick aggregate and in accordance with the ASTM C618 standard for pozzolanic materials, the material can be categorised as a class N pozzolan material. Recycled crushed brick aggregates can be used to reduce dead loads, efflorescence, and maintain good shape without maintenance, as well as reduce the cost of concrete. Crushed brick aggregates decrease the compressive and tensile strengths of concrete while increasing the compressive strength of mortar [35]. In a research conducted by P. Shewale et al. [36] to substitute natural sand with waste brick at 10 %, 20 %, and 30 % replacement ratios in fly ash and GGBS-based mortar, they found that the incorporation of waste brick aggregates reduced the compressive strength of the composites. Moreover, Khalil et al. [37] conducted a study to evaluate the use of brick aggregates to substitute natural sand at 10 %, 20 %, and 30 % ratios in geopolymer mortar based on metakaolin. They reported that an increase in brick aggregates lowered compressive strength, which can be attributable to the aggregate's lower strength and hardness compared to natural aggregates. Based on the research conducted by Hu et al. [31], the addition of recycled aggregate in fly ash/GGBS geopolymers had minimal impact on the mechanical performance of the mixture, even with increasing replacement ratios from 50 % to 100 %. Their study affirmed that the microstructure of the geopolymer matrix and the morphology of the matrix/aggregate interface remained largely unchanged after substituting natural aggregate with recycled aggregates. However, it was observed that the utilization of recycled aggregate resulted in a slight reduction in mechanical properties, primarily attributable to the higher presence of defects in recycled aggregates compared to natural counterparts.

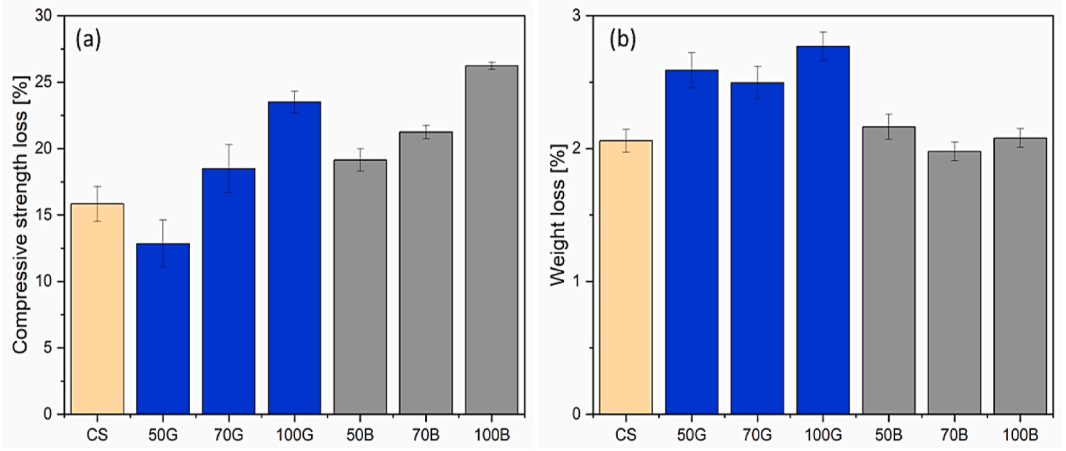

Fig. 8. (a) Compressive strength loss % and (b) weight loss % after freeze-thaw test.

3.2. Durability properties

3.2.1. Freeze-thaw assessment

The freeze-thaw (F-T) failure of a concrete structure occurs in three stages: water penetration, freezing, and structural collapses. At the stage of water absorption, external water enters the concrete through micro-cracks and fills the interior pores to near saturation. When the ambient temperature decreases to sub-zero degrees, the volume of frozen water swells by 9 %, and the inner wall of water-saturated pores undergoes tensile stress, leading to cracks and cement matrix spalling [38]. Fig. 8a and b illustrates the compressive strength and weight loss, following the 50 F-T cycles, the composites were weighed, and their compressive strengths were calculated and compared. As predicted, the weight and compressive strength of each composite decreased. 50G exhibited the lowest drop in compressive strength, by about 13 %, while 100B had the highest reduction, around 26 %. Control sample's compressive strength dropped by about 16 %. The compressive strength of 70G and 50B decreased by approximately 17 %, followed by 70B and 100G, which decreased by 21 % and 23 %, respectively (see Fig. 8-a). The weight loss of the investigated composites ranges from 2 % to 3 %, indicating their remarkable resistance to extreme temperature conditions (see Fig. 7-b). Notably, the compressive strength of composite 100B was measured at 33 MPa following the 50 F-T cycles, and it exhibited the highest compressive strength loss (26 %). This outcome provides further evidence of the composites' ability to function effectively in hostile environments. Regarding compressive strength loss, composites containing WGA performed better than those containing WBA across all replacement ratios. However, in terms of weight reduction, no clear pattern was observed among the composites. It's worth noting that brick made from pulverized clay is commonly considered a pozzolanic material. Pozzolans, when combined with water, interact with calcium hydroxide, resulting in the production of (CSH) and (CASH). This interaction enhances the properties of cement-based structures, providing further advantages to these composites [13,39]. Rheological characteristics of geopolymer are proportional to activator concentration and Si/Na molar ratio, and yield stress and viscosity will rise when increased. The extremely high ratio has the opposite effect, dissolving ions that are too late to react and preventing the creation of a network [40]. Subsequently, composites containing WBA and WGA undergo reaction, which may result in a high ratio of Si/Na has the opposite effect, scattering ions that are too slow to react and suppressing network development. Since various interacting characteristics influenced the matrix structures, it was difficult to comprehend the behaviour of composites when subjected to F-T cycles. In addition, to the best of the author's knowledge, no research has been conducted on WGA and WBA in AAM composites subjected to the freeze-thaw test.

3.2.2. Chloride attack assessment

The chloride attack on reinforced concrete is perhaps the most often seen and studied aspect of concrete's endurance. Through capillary absorption, hydrostatic pressure, and/or ion diffusion, chlorides are capable of penetrating. Chlorides stimulate the corrosion of embedded steel bars through a de-passivation process, resulting in a loss in the concrete's load-bearing capacity and possibly its structural collapse. Moreover, The predominant alkali-activation reaction products, namely C–A–S–H and N–A–S–H binding gels, which regulate ionic transport processes, have an effect on the chemistry and transport mechanisms of chloride in geopolymer mortar [41]. Fig. 9 depicts the reduction in compressive strength of composites after the execution of the chloride attack test. 100B had the lowest compressive strength loss of around 13 %, whereas 50G had the highest of approximately 28 %, while control sample's (CS) strength loss was 21 %. 100B outperformed CS by 62 %, while 50G trailed behind by 33 %. 70B exhibited the second-lowest compressive loss, at 17 %, which is superior to CS by 19 %. The compressive strength loss of 70G, 100G, and 50B was around 26 %, which was 24 % less than that of CS. Raising the replacement ratio of

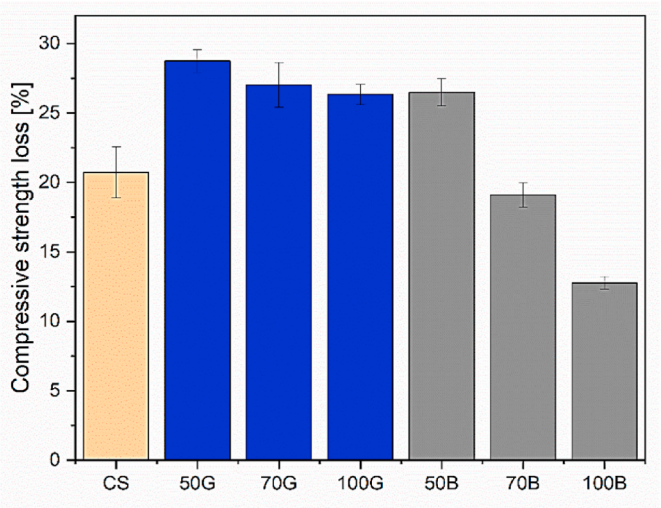

Fig. 9. Compressive strength loss % after chloride attack test.

natural sand with WBA significantly improved the chloride ingress resistance of the composite, whereas WGA had the reverse effect. Since WGA aggregates consist of fly ash, slag, and silica sand, which already reacted with alkali activators. The rheological properties of geopolymers are proportional to the alkali activator concentration and Si/Na molar ratio. If done correctly, increasing the Si/Na molar ratio could increase the rate of dissolution and polymerisation, leading to a rise in the yield stress and viscosity of geopolymers. Nevertheless, the super-high ratio has the contrasting effect, possibly because many ions that are late to react are dissolved, and their repulsion inhibits network formation [40] and this may have worked in favour of chloride ions penetration. On the other hand, the pozzolanic WBA had a significant impact on reducing the chloride ingress and eventually, minimizing compressive strength loss. These findings are supported by a few studies on Portland cement-based composites, which stated that the chloride content profiles reveal that concrete samples containing pozzolans had a considerably reduced chloride content at various periods and depths, particularly in deeper zones [42–44]. Moreover, the favourable effect the pozzolanic reaction of this pozzolan and, as a result, the consumption of calcium hydroxide, which results in an increase in tortuosity and a decrease in OH- in the pore solution. As a result, chloride ion conductivity and chloride penetration diminish [45]. This study revealed that composites containing 100B exhibited remarkable resistance to chloride penetration. Alkali-activated materials (AAMs) generally display lower chloride permeability compared to Portland/blend cements. However, there is currently no comprehensive database of chloride diffusion coefficients for AAMs. This discrepancy can be attributed to the fact that AAMs have been studied more extensively by materials scientists than by concrete technologists. Consequently, there remain unanswered questions regarding the accurate determination of these coefficients for non-Portland cements. This critical issue necessitates the attention and collaborative efforts of the scientific community to address and resolve [6].

3.2.3. Acid attack assessment

Acids in groundwater, chemical wastewater, or acids coming from the oxidation of sulphur compounds in backfill can attack and affect the durability of concrete substructure components. In addition, various concrete structures are vulnerable to acid rain erosion, particularly in industrial districts where sulfuric acid is frequently prevalent. Moreover, sulfuric acid corrodes sewer pipelines and waste treatment plants [46]. As illustrated in the outcomes presented in Fig. 10, both composites incorporating waste-derived aggregates exhibited superior performance compared to the control (refer to Fig. 10-a) in terms of compressive

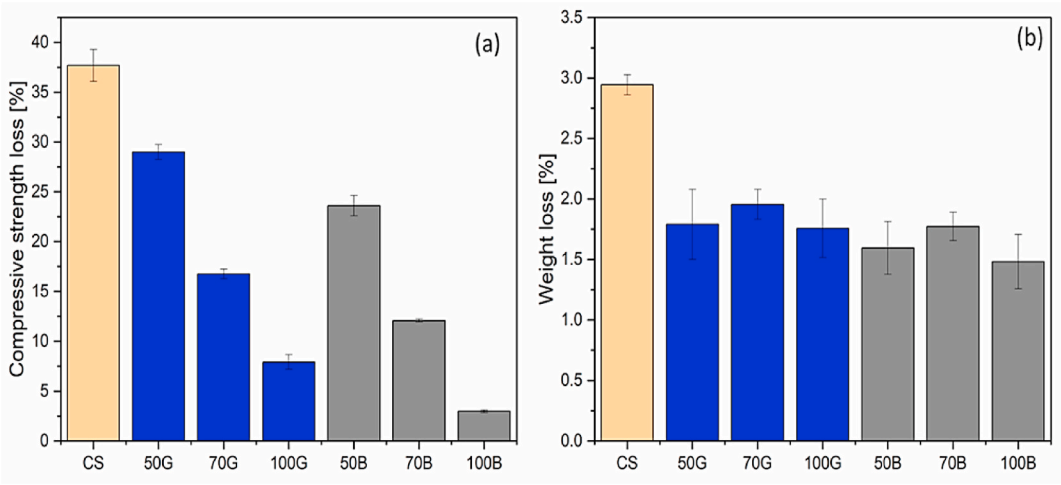

Fig. 10. (a) Compressive strength loss % and (b) weight loss % after acid attack test.

strength reduction. The incorporation of both WBA and WGA enhanced composites' acid attack resistivity. With the increase in incorporation aggregates, the loss of compressive strength decreased. Samples containing WBA performed better than samples containing WGA across every single replacement ratio in terms of compressive strength loss. 100B had the lowest drop in compressive strength, of around 2.5 %, while CS had the most, of approximately 37 %. 70B had the second-lowest reduction in compressive strength of about 12 %, followed by 50B of about 23 %. On the other hand, 50G, 70G, and 100G recorded compressive strength losses of about 28 %, 17 %, and 7 %, respectively. 100B was 93 % better than the control, while 50G was 24 % better in terms of comprehensive strength loss.

Fig. 10-b illustrated the composites' weight loss after performing the acid attack test. All samples containing WBA or WGA had a weight loss of less than 2 %, illustrating the composites strength against acid attack. On the contrary, the control's weight loss was about 3 %, which is higher than the rest of the composites and indicated that the loss was significant as it dropped the control's compressive strength by 37 %. In a study carried out by Izzat et al. (2013) [47] to examine OPC and geopolymer mortars, they stated that both mortars were shown to be susceptible to acidic attacks. The weight changes and the decrease in strength are consistent with this notion. Nevertheless, they affirmed that geopolymer specimens exhibited reduced susceptibility to acidic attack, as evidenced by weight changes and strength reductions of 3.6 % and 24 %, respectively. In contrast, OPC-based specimens experienced higher vulnerability with values of 18 % and 69 % for weight changes and strength reductions, respectively. It was proven that the durability performance of red clay brick waste/phosphorus slag-based geopolymer is related to its comparatively low calcium concentration and its extremely acid-resistant aluminosilicate composition. Moreover, acid attack resulted in significant calcium and sodium leaching into the acid solution, demonstrating the weak chemical link between calcium and sodium cations in the paste matrix. Existing unreacted brick particles in the matrix contribute to the low sodium content of the material, which is resistant to acid attack and exhibits a strong bonding type [48].

In a study carried out by Nuaklong et al. [49] where two types of fly ash were used, one with low calcium content and the other with high calcium content. They confirmed that a geopolymer-based substance with a low calcium content was less susceptible to degradation by a sulfuric acid solution, indicating that the presence of CaO in a geopolymer composite results in the synthesis of CSH and Ca (OH_2). A vigorous solution can quickly breakdown these calcium-based hydrated products. Moreover, Hafez et al. [50], stated that the alkali-activated-based mortar having 50 % fly ash, 35 % GGBS, and 15 % silica fume demonstrated greater resistance to magnesium sulphate than

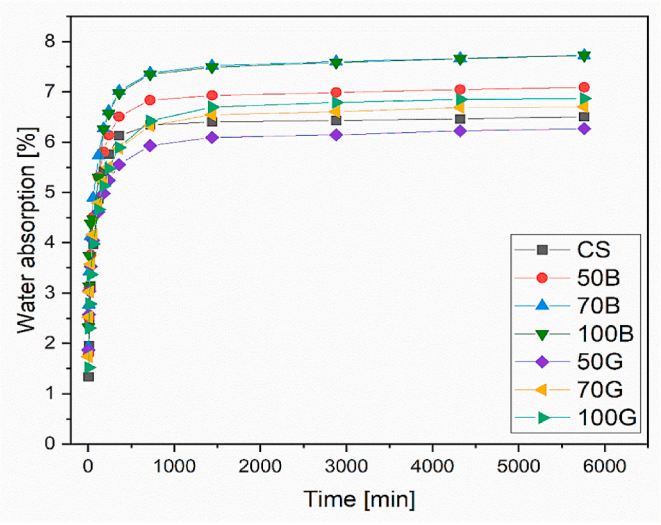

Fig. 11. Water absorption of AAM with waste brick and geo-cement aggregates at different replacement ratios.

mortar containing 100 % fly ash. The inclusion of WBA and WGA dramatically enhanced the composites acid attack resistance and proved their compatibility with the acid environment medium.

3.2.4. *Water absorption assessment*

Within the initial 8 h, the water absorption rates of all composites showed a distinct upward trend, followed by a stabilisation of the water absorption rate for all the composites (see Fig. 11). This pattern aligns, to some extent, with the ASTM C1585 [51] standard, although it's important to note that these composites are not OPC-based. The standard outlines two phases of capillary absorption: the primary phase occurring between the initial measurement and the one at 6 h, and the secondary phase spanning from the first measurement to the seventh day [52].70B and 100B samples had the highest water absorption rate, while the 50G sample had the lowest (see Fig. 11). At the 96-h mark, the water absorption for 70B and 100B measured approximately 8 %, while 50G showed a slightly lower rate at around 6 %, indicating an approximate 8 % reduction in water absorption compared to the control. The control, with the second-lowest water absorption rate, decreased to approximately 6.5 % after 96 h. In comparison, 70B and 100B exhibited water absorption rates about 25 % higher than the control. Following 96h, the water absorption rates of 70G, 100G, and 50B were, respectively, 6.6 %,

6.7 %, and 7 %, showing increases of about 1.5 %, 3 %, and 8 %, relative to the control. The results indicated that samples produced using waste brick aggregates had higher water absorption rates compared to samples prepared with geo-cement aggregates. This is due to the porous nature of recycled brick aggregates [53]. It's important to highlight that the laboratory testing of aggregates in this study revealed water absorption values of approximately 9.8 %, 8 %, and 7.5 % for WBA, sand, and WGA, respectively. The water absorption pattern observed in the incorporated composites mirrored that of the aggregates. Nonetheless, the variances in water absorption rates among the composites were comparable. Tavakoli et al. [18] reported that, in OPC-based composites, the amount of water that concrete can hold is equal to the sum of how much water cement paste and aggregates can hold. Since brick aggregates soak up more water than natural aggregates, this rise in water absorption was expected, which is in line with observations made in this work. Furthermore, Kasinikota et al. [54] validated the conclusions of this study by noting that the water absorption of samples based on Ordinary Portland Cement (OPC) rises with the increasing content of crushed brick waste, ranging from 8 % to 11 % as the dosage of crushed brick waste increases from 0 % to 24 %. Moreover, the percentage of brick powder in a gypsum-lime mortar increases the water absorption rate. Owing to the evaporation of the pooled water, the sample's porosity rises [55]. Priyanka et al. [56] reported that, the water absorption values were lower when the GGBS-base geopolymer aggregate replacement level was raised. As with time, GGBS's pozzolanic activity builds up. This means that there are fewer connections between voids, which makes it harder for water to get in. With an average particle size of 9.2 μm, GGBS particles fill all holes and small cracks, making concrete with fewer pores. A high GGBS surface area helps limit the aggregates' water absorption [40]. This finding explains why 50G had the lowest water absorption rate as it had better interlocking bond and less voids compared to 70G and 100G achieved higher water absorption rates. Further study is required to understand more about the microstructure of composites, as there is currently a scarcity of data on this topic. Yet, the fluctuations in water absorption rates of the mortar composites incorporated with WBA and WGA were tolerable. According to G. Golewski [57], water absorption of concrete below 10 % is already deemed minimal. The inclusion of WBA and WGA into AAM composites has intriguing effects in terms of water absorption.

4. Conclusions

The study focused on evaluating a versatile strategy for emission reduction in the global cement and concrete industries, utilising alkali-activation for low-carbon cement and incorporating waste-derived aggregates from bricks and geo-cement. Aiming to contribute to eco-sustainability in construction, the research assesses the engineering potential of these waste aggregates by analysing microstructure, mechanical performance, and durability properties, emphasising their substitution for virgin raw materials.

1. Specimens incorporating brick and geo-cement aggregates demonstrated mechanical performance, including flexural and compressive strengths, which either exceeded or were comparable to specimens with natural aggregates across all replacement ratios.
2. The surface roughness texture and angularity of brick and geo-cement aggregates exhibited compatibility, resulting in enhanced bonding with the matrix paste. Notably, the 50B and 70G samples showcased superior compressive (61 MPa) and flexural (12 MPa) strengths.
3. Incorporation of both brick and geo-cement aggregates in Alkali-Activated Materials (AAMs) exhibited enhanced resistance to acid attacks. Specifically, 100B and 100G showed minimal compressive strength losses of 2.5 % and 8 %, respectively, following an acid attack.
4. Among the evaluated mixes, 50G demonstrated the lowest water absorption rate and post-freeze-thaw compressive strength loss, registering values of 6 % and 13 %, respectively.
5. In the chloride attack test, 100B and 70B displayed the most favourable post-compressive strength losses at 13 % and 18 %, respectively.

Upon comprehensive analysis of the overall performance results across various tests, the recommended mixture is 50B, followed by 50G. Specifically, 50B exhibited a compressive strength of 61 MPa, flexural strength of 11 MPa, 26 % weight loss after the chloride test, a 7 % water absorption rate, and after the acid test, a 24 % compressive strength loss and 1.6 % weight loss. Furthermore, following freeze-thaw cycles, 50B displayed a 17 % compressive strength loss and a 2.2 % weight loss. Given the superior overall performance achieved with a 50 % replacement of both brick and geo-cement aggregates in Alkali-Activated Materials (AAM) composites, future investigations should focus on increasing the replacement ratio of waste aggregates while ensuring the maintenance of sufficient properties by either applying pretreatment to the aggregates or adding additives to the mix. Additionally, comprehensive assessments are necessary, considering the economic and environmental implications of incorporating waste aggregates into cementitious composites, along with technical and performance considerations. A rigorous evaluation of the economic feasibility of this study is imperative to gauge its potential for large-scale deployment and commercialisation.

CRediT authorship contribution statement

Eslam El-Seidy: Data curation, Investigation, Methodology, Writing - original draft, Writing - review & editing. **Mehdi Chougan:** Conceptualization, Data curation, Formal analysis, Writing - original draft. **Yazeed A. Al-Noaimat:** Data curation, Investigation. **Mazen J. Al-Kheetan:** Formal analysis, Writing - original draft. **Seyed Hamidreza Ghaffar:** Conceptualization, Formal analysis, Funding acquisition, Investigation, Resources, Supervision, Validation, Writing - original draft.

Declaration of competing interest

The authors declare that they have no known competing financial interests or personal relationships that could have appeared to influence the work reported in this paper.

Data availability

Data will be made available on request.

Acknowledgement

This work was funded as part of the DigiMat project, which has received funding from the European Union's Horizon 2020 research and innovation program under the Marie Skłodowska-Curie grant agreement ID: 101029471.

References

[1] J. Kirchherr, D. Reike, M. Hekkert, Conceptualizing the circular economy: an analysis of 114 definitions, Resour. Conserv. Recycl. 127 (2017) 221–232, https://doi.org/10.1016/j.resconrec.2017.09.005.
[2] K.Y.G. Kwok, J. Kim, A.M. Asce, W.K.O. Chong, M. Asce, S.T. Ariaratnam, F. Asce, Structuring a Comprehensive Carbon-Emission Framework for the Whole Lifecycle of Building, Operation, and Construction, 2016, https://doi.org/10.1061/(ASCE)AE.1943-5568.0000215.
[3] E. Benhelal, E. Shamsaei, M.I. Rashid, Challenges against CO2 abatement strategies in cement industry: a review, J. Environ. Sci. 104 (2021) 84–101, https://doi.org/10.1016/j.jes.2020.11.020.

[4] L. Proaño, A.T. Sarmiento, M. Figueredo, M. Cobo, Techno-economic evaluation of indirect carbonation for CO2 emissions capture in cement industry: a system dynamics approach, J. Clean. Prod. 263 (2020), https://doi.org/10.1016/j.jclepro.2020.121457.

[5] J.L. Provis, S.A. Bernal, Geopolymers and related alkali-activated materials, Annu. Rev. Mater. Res. 44 (2014) 299–327, https://doi.org/10.1146/annurev-matsci-070813-113515.

[6] S.A. Bernal, J.L. Provis, Durability of alkali-activated materials: progress and perspectives, J. Am. Ceram. Soc. 97 (2014) 997–1008, https://doi.org/10.1111/jace.12831.

[7] Y. Zhang, W. Luo, J. Wang, Y. Wang, Y. Xu, J. Xiao, A review of life cycle assessment of recycled aggregate concrete, Constr. Build. Mater. 209 (2019) 115–125, https://doi.org/10.1016/j.conbuildmat.2019.03.078.

[8] J. Shi, J. Tan, B. Liu, J. Chen, J. Dai, Z. He, Experimental study on full-volume slag alkali-activated mortars: air-cooled blast furnace slag versus machine-made sand as fine aggregates, J. Hazard Mater. 403 (2021) 123983, https://doi.org/10.1016/j.jhazmat.2020.123983.

[9] B.C. Mendes, L.G. Pedroti, C.M.F. Vieira, M. Marvila, A.R.G. Azevedo, J.M. Franco de Carvalho, J.C.L. Ribeiro, Application of eco-friendly alternative activators in alkali-activated materials: a review, J. Build. Eng. 35 (2021), https://doi.org/10.1016/j.jobe.2020.102010.

[10] I. Almeshal, B.A. Tayeh, R. Alyousef, H. Alabduljabbar, A. Mustafa Mohamed, A. Alaskar, Use of recycled plastic as fine aggregate in cementitious composites: a review, Constr. Build. Mater. 253 (2020) 119146, https://doi.org/10.1016/j.conbuildmat.2020.119146.

[11] K. Kabirifar, M. Mojtahedi, C. Wang, V.W.Y. Tam, Construction and demolition waste management contributing factors coupled with reduce, reuse, and recycle strategies for effective waste management: a review, J. Clean. Prod. 263 (2020) 121265, https://doi.org/10.1016/j.jclepro.2020.121265.

[12] H. Ilcan, O. Sahin, A. Kul, E. Ozcelikci, M. Sahmaran, Rheological property and extrudability performance assessment of construction and demolition waste-based geopolymer mortars with varied testing protocols, Cem. Concr. Compos. 136 (2023) 104891, https://doi.org/10.1016/J.CEMCONCOMP.2022.104891.

[13] C.L. Wong, K.H. Mo, S.P. Yap, U.J. Alengaram, T.C. Ling, Potential use of brick waste as alternate concrete-making materials: a review, J. Clean. Prod. 195 (2018) 226–239, https://doi.org/10.1016/j.jclepro.2018.05.193.

[14] K. Rashid, E.U. Haq, M.S. Kamran, N. Munir, A. Shahid, I. Hanif, Experimental and finite element analysis on thermal conductivity of burnt clay bricks reinforced with fibers, Constr. Build. Mater. 221 (2019) 190–199, https://doi.org/10.1016/J.CONBUILDMAT.2019.06.055.

[15] Z. He, A. Shen, H. Wu, W. Wang, L. Wang, C. Yao, J. Wu, Research progress on recycled clay brick waste as an alternative to cement for sustainable construction materials, Constr. Build. Mater. 274 (2021) 122113, https://doi.org/10.1016/j.conbuildmat.2020.122113.

[16] M. Ngoc-Tra Lam, D.-H. Le, D.-L. Nguyen, Reuse of clay brick and ceramic waste in concrete: a study on compressive strength and durability using the Taguchi and Box–Behnken design method, Constr. Build. Mater. 373 (2023) 130801, https://doi.org/10.1016/j.conbuildmat.2023.130801.

[17] S. Mesgari, A. Akbarnezhad, J.Z. Xiao, Recycled geopolymer aggregates as coarse aggregates for Portland cement concrete and geopolymer concrete: effects on mechanical properties, Constr. Build. Mater. 236 (2020) 117571, https://doi.org/10.1016/j.conbuildmat.2019.117571.

[18] D. Tavakoli, P. Fakharian, J. de Brito, Mechanical properties of roller-compacted concrete pavement containing recycled brick aggregates and silica fume, Road Mater. Pavement Des. 23 (2022) 1793–1814, https://doi.org/10.1080/14680629.2021.1924236.

[19] M.M. Atyia, M.G. Mahdy, M. Abd Elrahman, Production and properties of lightweight concrete incorporating recycled waste crushed clay bricks, Constr. Build. Mater. 304 (2021) 124655, https://doi.org/10.1016/j.conbuildmat.2021.124655.

[20] C. Wang, J. Xiao, W. Liu, Z. Ma, Unloading and reloading stress-strain relationship of recycled aggregate concrete reinforced with steel/polypropylene fibers under uniaxial low-cycle loadings, Cem. Concr. Compos. 131 (2022) 104597, https://doi.org/10.1016/J.CEMCONCOMP.2022.104597.

[21] C. Wang, H. Wu, C. Li, Hysteresis and damping properties of steel and polypropylene fiber reinforced recycled aggregate concrete under uniaxial low-cycle loadings, Constr. Build. Mater. 319 (2022) 126191, https://doi.org/10.1016/J.CONBUILDMAT.2021.126191.

[22] C. Wang, J. Xiao, C. Qi, C. Li, Rate sensitivity analysis of structural behaviors of recycled aggregate concrete frame, J. Build. Eng. 45 (2022) 103634, https://doi.org/10.1016/J.JOBE.2021.103634.

[23] E. El-Seidy, M. Sambucci, M. Chougan, M.J. Al-Kheetan, I. Biblioteca, M. Valente, S.H. Ghaffar, Mechanical and physical characteristics of alkali- activated mortars incorporated with recycled polyvinyl chloride and rubber aggregates, J. Build. Eng. 60 (2022) 105043, https://doi.org/10.1016/j.jobe.2022.105043.

[24] E. El-Seidy, M. Chougan, M. Sambucci, M.J. Al-Kheetan, I. Biblioteca, M. Valente, S. Hamidreza Ghaffar, Lightweight Alkali-Activated Materials and Ordinary Portland Cement Composites Using Recycled Polyvinyl Chloride and Waste Glass Aggregates to Fully Replace Natural Sand, 2023, https://doi.org/10.1016/j.conbuildmat.2023.130399.

[25] B. Panda, M.J. Tan, Rheological behavior of high volume fly ash mixtures containing micro silica for digital construction application, Mater. Lett. 237 (2019) 348–351, https://doi.org/10.1016/j.matlet.2018.11.131.

[26] M. Chougan, S. Hamidreza Ghaffar, M. Jahanzat, A. Albar, N. Mujaddedi, R. Swash, The influence of nano-additives in strengthening mechanical performance of 3D printed multi-binder geopolymer composites, (n.d.). https://doi.org/10.1016/j.conbuildmat.2020.118928.

[27] E. El-seidy, M. Sambucci, M. Chougan, Y.A. Ai-noaimat, M.J. Al-kheetan, I. Biblioteca, M. Valente, S. Hamidreza, Alkali activated materials with recycled unplasticised polyvinyl chloride aggregates for sand replacement, Constr. Build. Mater. 409 (2023) 134188, https://doi.org/10.1016/j.conbuildmat.2023.134188.

[28] M. Moranville, S. Kamali, E. Guillon, Physicochemical equilibria of cement-based materials in aggressive environments—experiment and modeling, Cem. Concr. Res. 34 (2004) 1569–1578.

[29] B.S. EN, 1097-6, Tests for Mechanical and Physical Properties of Aggregates, Determ. Part, Density Water Absorption, BSI, 2013.

[30] P. Zhu, M. Hua, H. Liu, X. Wang, C. Chen, Interfacial evaluation of geopolymer mortar prepared with recycled geopolymer fine aggregates, Constr. Build. Mater. 259 (2020) 119849, https://doi.org/10.1016/j.conbuildmat.2020.119849.

[31] G. Santha Kumar, Influence of fluidity on mechanical and permeation performances of recycled aggregate mortar, Constr. Build. Mater. 213 (2019) 404–412, https://doi.org/10.1016/j.conbuildmat.2019.04.093.

[32] S. Iftikhar, K. Rashid, E. Ul Haq, I. Zafar, F.K. Alqahtani, M. Iqbal Khan, Synthesis and characterization of sustainable geopolymer green clay bricks: an alternative to burnt clay brick, Constr. Build. Mater. 259 (2020) 119659, https://doi.org/10.1016/J.CONBUILDMAT.2020.119659.

[33] M. Khattab, S. Hachemi, M. Fawzi, A. Ajlouni, The use of recycled aggregate from waste refractory brick for the future of sustainable concrete, Int. Congr. Phenomenol. Asp. Civ. Eng. (2021) 1–6.

[34] O.M. Olofinnade, J.I. Ogara, I.T. Oyawoye, A.N. Ede, J.M. Ndambuki, K. D. Oyeyemi, D.O. Nduka, Mechanical properties of high strength eco-concrete containing crushed waste clay brick aggregates as replacement for sand, IOP Conf. Ser. Mater. Sci. Eng. 640 (2019), https://doi.org/10.1088/1757-899X/640/1/012046.

[35] F.S. Klak, H. Saleh, A.S. Tais, Recycling of crushed clay bricks as fine aggregate in concrete and cement mortar, Aust. J. Struct. Eng. 00 (2022) 1–10, https://doi.org/10.1080/13287982.2022.2098600.

[36] P. Shewale, P. Thorat, A. Bagat, A. Patil, R. Khaware, M. Kamble, S.B. Pawar, Experimental study on assessment of fly ash and GGBS based geopolymer mortar with brick waste replacement to fine aggregates, Int. Res. J. Eng. Technol. (2022) 1392–1398. www.irjet.net.

[37] W.I. Khalil, Q.J. Frayyeh, M.F. Ahmed, Evaluation of sustainable metakaolin-geopolymer concrete with crushed waste clay brick, IOP Conf. Ser. Mater. Sci. Eng. 518 (2019), https://doi.org/10.1088/1757-899X/518/2/022053.

[38] R. Wang, Z. Hu, Y. Li, K. Wang, H. Zhang, Review on the deterioration and approaches to enhance the durability of concrete in the freeze–thaw environment, Constr. Build. Mater. 321 (2022) 126371, https://doi.org/10.1016/j.conbuildmat.2022.126371.

[39] L. Reig, M.M. Tashima, M.V. Borrachero, J. Monzó, C.R. Cheeseman, J. Payá, Properties and microstructure of alkali-activated red clay brick waste, Constr. Build. Mater. 43 (2013) 98–106, https://doi.org/10.1016/j.conbuildmat.2013.01.031.

[40] J. Zhao, L. Tong, B. Li, T. Chen, C. Wang, G. Yang, Y. Zheng, Eco-friendly geopolymer materials: a review of performance improvement, potential application and sustainability assessment, J. Clean. Prod. 307 (2021) 127085, https://doi.org/10.1016/J.JCLEPRO.2021.127085.

[41] I. Ismail, S.A. Bernal, J.L. Provis, R. San Nicolas, D.G. Brice, A.R. Kilcullen, S. Hamdan, J.S.J. Van Deventer, Influence of fly ash on the water and chloride permeability of alkali-activated slag mortars and concretes, Constr. Build. Mater. 48 (2013) 1187–1201, https://doi.org/10.1016/j.conbuildmat.2013.07.106.

[42] M.H. Tadayon, M. Shekarchi, M. Tadayon, Long-term field study of chloride ingress in concretes containing pozzolans exposed to severe marine tidal zone, Constr. Build. Mater. 123 (2016) 611–616, https://doi.org/10.1016/j.conbuildmat.2016.07.074.

[43] R. Vedalakshmi, K. Rajagopal, N. Palaniswamy, Longterm corrosion performance of rebar embedded in blended cement concrete under macro cell corrosion condition, Constr. Build. Mater. 22 (2008) 186–199, https://doi.org/10.1016/j.conbuildmat.2006.09.004.

[44] X. Shi, N. Xie, K. Fortune, J. Gong, Durability of steel reinforced concrete in chloride environments: an overview, Constr. Build. Mater. 30 (2012) 125–138, https://doi.org/10.1016/j.conbuildmat.2011.12.038.

[45] K. Samimi, S. Kamali-Bernard, A. Akbar Maghsoudi, M. Maghsoudi, H. Siad, Influence of pumice and zeolite on compressive strength, transport properties and resistance to chloride penetration of high strength self-compacting concretes, Constr. Build. Mater. 151 (2017) 292–311, https://doi.org/10.1016/j.conbuildmat.2017.06.071.

[46] H. Janfeshan Araghi, I.M. Nikbin, S. Rahimi Reskati, E. Rahmani, H. Allahyari, An experimental investigation on the erosion resistance of concrete containing various PET particles percentages against sulfuric acid attack, Constr. Build. Mater. 77 (2015) 461–471, https://doi.org/10.1016/j.conbuildmat.2014.12.037.

[47] A.M. Izzat, A.M.M. Al Bakri, H. Kamarudin, L.M. Moga, G.C.M. Ruzaidi, M.T. M. Faheem, A.V. Sandu, Microstructural analysis of geopolymer and ordinary Portland cement mortar exposed to sulfuric acid, Mater. Plast. 50 (2013) 171–174.

[48] M. Vafaei, A. Allahverdi, P. Dong, N. Bassim, M. Mahinroosta, Resistance of red clay brick waste/phosphorus slag-based geopolymer mortar to acid solutions of mild concentration, J. Build. Eng. 34 (2021) 102066, https://doi.org/10.1016/j.jobe.2020.102066.

[49] P. Nuaklong, A. Wongsa, V. Sata, K. Boonserm, J. Sanjayan, Heliyon Properties of high-calcium and low-calcium fl y ash combination geopolymer mortar containing recycled aggregate, Heliyon 5 (2019) e02513, https://doi.org/10.1016/j.heliyon.2019.e02513.

[50] H.E. Elyamany, A. Elmoaty, M.A. Elmoaty, A. Rahman, Sulphuric acid resistance of slag geopolymer concrete modified with fly ash and silica fume, Iran, J. Sci. Technol. Trans. Civ. Eng. 45 (2021) 2297–2315, https://doi.org/10.1007/s40996-020-00515-5.

[51] ASTM-C1585 | Standard Test Method for Measurement of Rate of Absorption of Water by Hydraulic-Cement Concretes | Document Center, Inc., (n.d.). https://www.document-center.com/standards/show/ASTM-C1585 (accessed December 16, 2023).

[52] M. Frías, M. Monasterio, J. Moreno-Juez, Physical and mechanical behavior of new ternary and hybrid eco-cements made from construction and demolition waste, Materials 16 (2023), https://doi.org/10.3390/ma16083093.

[53] B. Debnath, P. Pratim Sarkar, Quantification of random pore features of porous concrete mixes prepared with brick aggregate: an application of stereology and mathematical morphology, Constr. Build. Mater. 294 (2021) 123594, https://doi.org/10.1016/j.conbuildmat.2021.123594.

[54] P. Kasinikota, D.D. Tripura, Evaluation of compressed stabilized earth block properties using crushed brick waste, Constr. Build. Mater. 280 (2021) 122520, https://doi.org/10.1016/j.conbuildmat.2021.122520.

[55] K. Naciri, I. Aalil, A. Chaaba, Eco-friendly gypsum-lime mortar with the incorporation of recycled waste brick, Constr. Build. Mater. 325 (2022) 126770, https://doi.org/10.1016/j.conbuildmat.2022.126770.

[56] M. Priyanka, K. Muniraj, S.R.C. Madduru, Influence of geopolymer aggregates on micro-structural and durability characteristics of OPC concrete, J. Build. Pathol. Rehabil. 7 (2022) 1–16, https://doi.org/10.1007/s41024-021-00153-y.

[57] G.L. Golewski, Assessing of water absorption on concrete composites containing fly ash up to 30 % in regards to structures completely immersed in water, Case Stud. Constr. Mater. 19 (2023) e02337, https://doi.org/10.1016/J.CSCM.2023.E02337.